Cell, Vol. 108, 649–660, March 8, 2002, Copyright ©2002 by Cell Press

A Ca^{2+} Switch Aligns the Active Site of Calpain

Tudor Moldoveanu, Christopher M. Hosfield, Daniel Lim, John S. Elce, Zongchao Jia, and Peter L. Davies[1]
Department of Biochemistry and the Protein Engineering Network of Centres of Excellence
Queen's University
Kingston, Ontario K7L 3N6
Canada

Summary

Ca^{2+} signaling by calpains leads to controlled proteolysis during processes ranging from cytoskeleton remodeling in mammals to sex determination in nematodes. Deregulated Ca^{2+} levels result in aberrant proteolysis by calpains, which contributes to tissue damage in heart and brain ischemias as well as neurodegeneration in Alzheimer's disease. Here we show that activation of the protease core of μ calpain requires cooperative binding of two Ca^{2+} atoms at two non-EF-hand sites revealed in the 2.1 Å crystal structure. Conservation of the Ca^{2+} binding residues defines an ancestral general mechanism of activation for most calpain isoforms, including some that lack EF-hand domains. The protease region is not affected by the endogenous inhibitor, calpastatin, and may contribute to calpain-mediated pathologies when the core is released by autoproteolysis.

Introduction

The calpains form a superfamily of intracellular cysteine proteases with numerous isoforms in organisms ranging from mammals to *Drosophila melanogaster* and *Caenorhabditis elegans* and with homologs in yeast and bacteria (Sorimachi and Suzuki, 2001). They function in Ca^{2+} signaling by modulating biological activities of their substrates through limited proteolysis (Glading et al., 2002; Carafoli and Molinari, 1998; Sorimachi et al., 1997). The mammalian heterodimeric μ and m calpains are the most extensively studied isoforms and have been implicated in cell motility (Cox and Huttenlocher, 1998), apoptosis (Wang, 2000), cell cycle progression (Santella et al., 1998), and development (Arthur et al., 2000; Zimmerman et al., 2000). One of the best-documented functions for these enzymes is the regulation of integrin-mediated cell migration. Here calpains release the link between the integrin-dependent focal adhesion complex and the actin cytoskeleton by proteolysis of talin, which allows proper cell migration. Mouse embryonic fibroblasts from the developmentally lethal calpain small subunit knockout (Arthur et al., 2000) lack detectable calpain activity and show heavily impaired cell migration, because intact talin prevents the proper release of focal adhesions from actin stress fibers (Dourdin et al., 2001). The balance between calpain and its endogenous inhibitors like calpastatin and Gas-2 is critical for normal physiological function. Overproduction of m calpain during v-Src signaling promotes cleavage of focal adhesion kinase, resulting in disassembly of the focal adhesion complex and progression to the transformed phenotype (Carragher et al., 2002). Overproduction of the Gas2 inhibitor blocks m calpain-directed p53 degradation and thus promotes apoptosis (Benetti et al., 2001).

The role of calpains in several pathologies is well documented. Limb girdle muscular dystrophy 2A (LGMD2A) is a disease caused by mutations in the muscle-specific calpain p94 (Richard et al., 1995), some of which were shown to cause loss of enzyme function (Ono et al., 1998). On the other hand, hyperactivation of calpain due to elevated cellular Ca^{2+} levels contributes to tissue damage seen during ischemic injury to the heart (Wang and Yuen, 1994) and brain (Lee et al., 1997) and during neurodegeneration (Nixon, 2000). In Alzheimer's disease, amyloid peptides induce aberrant calpain activation that results in mislocalization of cyclin-dependent kinase 5 (cdk5) due to proteolytic processing of the cdk5-related cyclin p35 to p25 (Patrick et al., 1999; Lee et al., 2000). Deregulated cdk5 hyperphosphorylates tau, which promotes neuronal death. Administration of calpain inhibitors has been shown to lessen or prevent tissue damage, but the toxicity and lack of specificity of current inhibitors weakens the effectiveness of such therapies (Wang and Yuen, 1994).

Elucidation of the pathophysiological roles of calpains requires an understanding of their regulation by Ca^{2+} at the molecular level. The crystal structures of Ca^{2+}-free m calpain heterodimer (Hosfield et al., 1999; Strobl et al., 2000) showed how domains DI and II are held slightly apart and rotated, so that the catalytic triad residues are not correctly aligned. It was hypothesized that this misalignment was due to constraints imposed by the circular arrangement of domains. The anchor peptide (~20 residues) at the N terminus of the large subunit (80 kDa) interacts with the small subunit DVI (21 kDa) to restrain DI, while the C2-like DIII restricts DII. The trigger for constraint release was suggested to be Ca^{2+} binding to the EF-hand-containing DIV and DVI. However, in the absence of a Ca^{2+} bound crystal structure, the mechanism of activation of the heterodimers remained speculative (Sorimachi and Suzuki, 2001).

The structural and biochemical data presented here suggest that the protease core of μ calpain (μI-II), which lacks both the EF-hand and C2-like domains, retains the minimal functional and structural requirements of a Ca^{2+}-dependent cysteine protease. It binds Ca^{2+} at two conserved sites, suggesting that the mechanism of activation for this minicalpain applies to most isoforms in the diverse family of Ca^{2+}-dependent cysteine proteases. Moreover, the Ca^{2+} bound μI-II structure provides an ideal target for design and testing of active site inhibitors that will help delineate the pathophysiological roles of the calpains.

[1]Correspondence: daviesp@post.queensu.ca

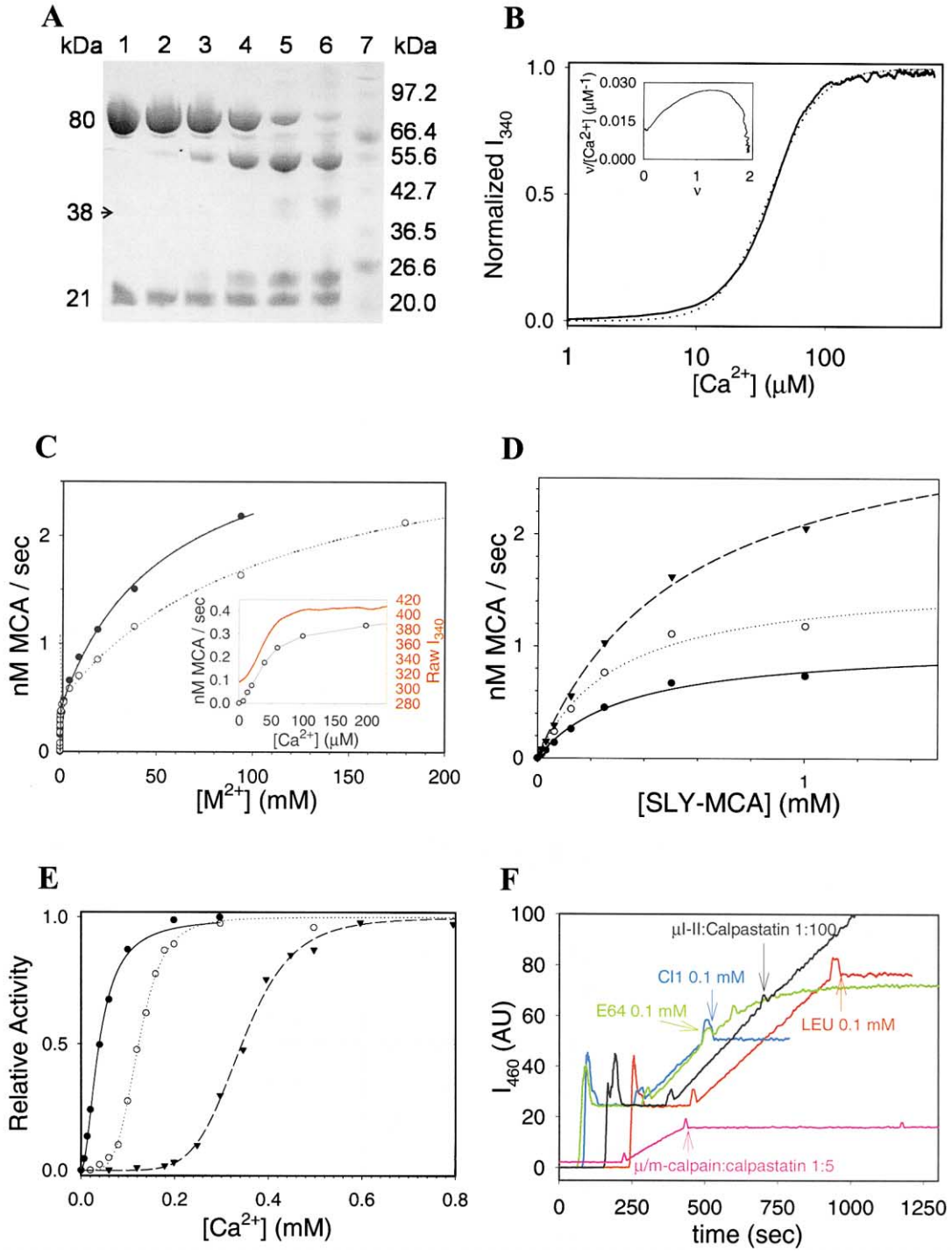

Figure 1. Ca^{2+}-Dependent Protease Activity and Conformational Change of μI-II

(A) SDS-PAGE analysis of μI-II-digested calpain. Proteolysis of inactive recombinant m calpain heterodimer (C105S-m80k/21k) by μI-II (38 kDa) was performed in the presence of 1 mM $CaCl_2$ at an enzyme to substrate molar ratio of 1:25 as described in Experimental Procedures. Lanes 1–6 contained aliquots of the reaction that were digested for 0, 5, 20, 80, 320 min, and 20 hr, respectively. Lane 7 contained the molecular weight markers (kDa).

(B) Ca^{2+}-induced conformational change in μI-II. Intrinsic fluorescence intensity was monitored at 340 nm (I_{340}) by exciting μI-II at 280 nm while continuously adding $CaCl_2$. The Hill equation (dotted line) was fitted to a semilogarithmic plot of the normalized intensity (solid line). Positive cooperativity between sites is shown in the inset by the upward curved Scatchard plot; ν is the fraction of total number of sites that are bound.

(C) Divalent cation (M^{2+}) effects on μI-II activity. Increasing concentrations of $CaCl_2$ (●) or $MgCl_2$ (○) were added to 2.5 μM μI-II in the presence of 0.25 mM SLY-MCA. All assays with $MgCl_2$ were done in the presence of 1 mM $CaCl_2$. At low $CaCl_2$ concentrations, enzyme activity (black line) and tryptophan fluorescence (red line) profiles were both sigmoidal (inset).

Results

μI-II as a Minicalpain

A construct containing only the active site domains I-II was expected to be free of restraining interactions from neighboring regions and might therefore function in the absence of Ca^{2+}. We showed, however, that recombinant μI-II is completely lacking in proteolytic activity in the absence of Ca^{2+}, but is active in the presence of Ca^{2+} (Figure 1). Calpain is a natural substrate for itself, as demonstrated by autolysis (Crawford et al., 1993; Nishimura and Goll, 1991; Tompa et al., 1996). At an enzyme to substrate molar ratio of 1:25 and in the presence of 1 mM $CaCl_2$, μI-II cleaved the large subunit of the inactive m calpain heterodimer C105S-m80k/21k (Elce et al., 1995) to generate 55 kDa, 40 kDa, and 24 kDa fragments (Figure 1A). No proteolysis was observed without Ca^{2+} or when Mg^{2+} or other divalent cations were substituted for Ca^{2+} (not shown). Moreover, the digestion profile strongly resembled the usual m calpain autolysis profile (Crawford et al., 1993), suggesting similar substrate specificities for μI-II and for intact calpain. Compared to intact m or μ calpain, the μI-II construct is weakly active at 1 mM $CaCl_2$, because digestion of the large subunit (80 kDa) was incomplete after 20 hr (Figure 1A) compared to ~40 min for the intact enzymes (not shown).

Activation of μI-II by Ca^{2+} led us to look for a Ca^{2+}-induced conformational change by means of intrinsic tryptophan fluorescence. A sigmoidal increase in intrinsic fluorescence was observed with increasing Ca^{2+} concentration (Figure 1B). The data fit readily to the Hill equation (Hill coefficient 1.88 ± 0.35), suggesting that Ca^{2+} binding involves more than one site and that these sites are positively cooperative. This was shown by the upward curvature of the Scatchard plot (Figure 1B, inset). The total increase in fluorescence intensity was 36.8% ± 0.5% (Figure 1C, inset), with the increase being first detectable at ~5 μM $CaCl_2$ and ~90% complete at ~100 μM $CaCl_2$. The change was completely reversed by EDTA (not shown). The half-maximal change in fluorescence occurred at 41.8 ± 7.1 μM $CaCl_2$, which falls in the range of values reported for half-maximal activation of intact μ calpain (5–50 μM; Croall and DeMartino, 1991). $MgCl_2$, $MnCl_2$, and $ZnCl_2$, even at concentrations up to 30 mM, had no effect.

When assayed with the common calpain substrate SLY-MCA, μI-II was active only in the presence of $CaCl_2$ (Figures 1C and 1D) and not with $MgCl_2$, $MnCl_2$, or $ZnCl_2$ even at concentrations up to 30 mM (not shown). μI-II activity showed a biphasic $CaCl_2$ titration. At concentrations below 0.5 mM, the sigmoidal activity increase was strictly Ca^{2+}-dependent and correlated with the increase in tryptophan fluorescence (Figure 1C, inset). At the end of this sigmoidal phase, the kinetic parameters for SLY-MCA hydrolysis in the presence of 0.5 mM $CaCl_2$ (K_M = 0.335 ± 0.006 mM, k_{cat} = 4.27 ± 0.47 × 10^{-4} s^{-1}; Figure 1D) indicate that μI-II is weakly active compared to intact m calpain (K_M = 0.212 ± 0.017 mM, k_{cat} = 0.016 ± 0.001 s^{-1}), mainly due to a 37.5-fold lower turnover number (k_{cat}). Addition of more $CaCl_2$ (Figure 1C) resulted in a hyperbolic increase in activity (Figure 1C) but no further change in tryptophan fluorescence. The k_{cat} increased to 6.10 ± 0.52 × 10^{-4} s^{-1} at 5 mM $CaCl_2$ and to 1.29 ± 0.07 × 10^{-3} s^{-1} at 20 mM $CaCl_2$, while K_M values remained fairly constant (Figure 1D). Only during this second phase could $MgCl_2$ (and to a lesser extent NaCl) substitute for $CaCl_2$ (Figure 1C). The nonspecific effect of these salts was to raise the turnover number for μI-II to ~1/3 that of m calpain (at >100 mM $CaCl_2$; Figure 1C).

To help assess the role of the other domains in the activation process, we replaced DI-II of m calpain with μI-II to make a μ/m calpain hybrid. This hybrid has very similar kinetic properties to m80k/21k calpain (K_M for SLY-MCA hydrolysis = 0.217 ± 0.016 mM, k_{cat} = 0.018 ± 0.001 s^{-1}). Its $CaCl_2$ requirement for half-maximal activation (121 μM) was intermediate between those for m calpain (343 μM) and for the sigmoidal phase of μI-II activation (46 μM; Figure 1E).

Interestingly, μI-II was not inhibited by a ≤100-fold excess of recombinant calpastatin domain I (Figure 1F). This 140 residue protein has been previously shown to inhibit calpain, and it completely blocked μ/m calpain hybrid activity at an enzyme to inhibitor ratio of 1:5 (Figure 1F). However, μI-II was completely inhibited by a 40-fold molar excess of E64, leupeptin, and calpain inhibitor I (Figure 1F), suggesting that the active site conformation in μI-II is very similar to that of the protease region in the intact enzyme.

Overall Structure

The Ca^{2+} bound crystal structure of C115S μI-II shows a compact molecule, approximately 70 × 40 × 35 Å, formed by a tight association of DI and II (Figure 2A). Over 85% of the residues form essentially the same structure as DI-II from the inactive m calpain heterodimer (Hosfield et al., 1999; Strobl et al., 2000), with the rest being noticeably different. DI maintains the core α helix (α5) surrounded by two β sheets (β2, 5, 6 and β1, 3, 4) on one side and a cluster of α helices (α3, 4, 6) on the other side. DII maintains two antiparallel β sheets (β7, 8, 14 and β11, 12, 13) that form the core of the inactive structure. The presence of two Ca^{2+} ions, one bound in each domain, and the relative orientation of the two domains define the two most significant structural differences between the active and inactive states. Both

(D) Michaelis-Menten analysis of the hydrolysis of the synthetic peptide SLY-MCA. Increasing concentrations of SLY-MCA were digested by 2.5 μM μI-II in the presence of 0.5 (●), 5 (○), and 20 (▼) mM $CaCl_2$. Representative Michaelis-Menten plots are shown.

(E) Calpain activity as a function of $CaCl_2$ concentration. Initial reaction rates for SLY-MCA hydrolysis by μI-II (●), μ/m calpain (○), and m80k/21k (▼) at varying $CaCl_2$ concentrations were normalized and fitted to the Hill equation plot.

(F) Effect of calpain inhibitors on the hydrolysis of SLY-MCA. Hydrolysis of 0.4 mM SLY-MCA in 0.5 mM $CaCl_2$ was assayed under the same conditions used for steady-state kinetic analysis in Figure 1D. The reaction was started by the addition of Ca^{2+}. The addition of the inhibitors CI1 (calpain inhibitor 1, N-acetyl-Leu-Leu-Norleucinal), E64 (trans-epoxysuccinyl-L-leucylamido-(4-guanidino)-butane), LEU (Leupeptin, N-acetyl-Leu-Leu-Argininal), and recombinant rat calpastatin (domain I) is indicated by arrows on the red, green, blue, and black traces, respectively. μ/m calpain inhibition by calpastatin is indicated in pink. Enzyme to inhibitor ratios are molar.

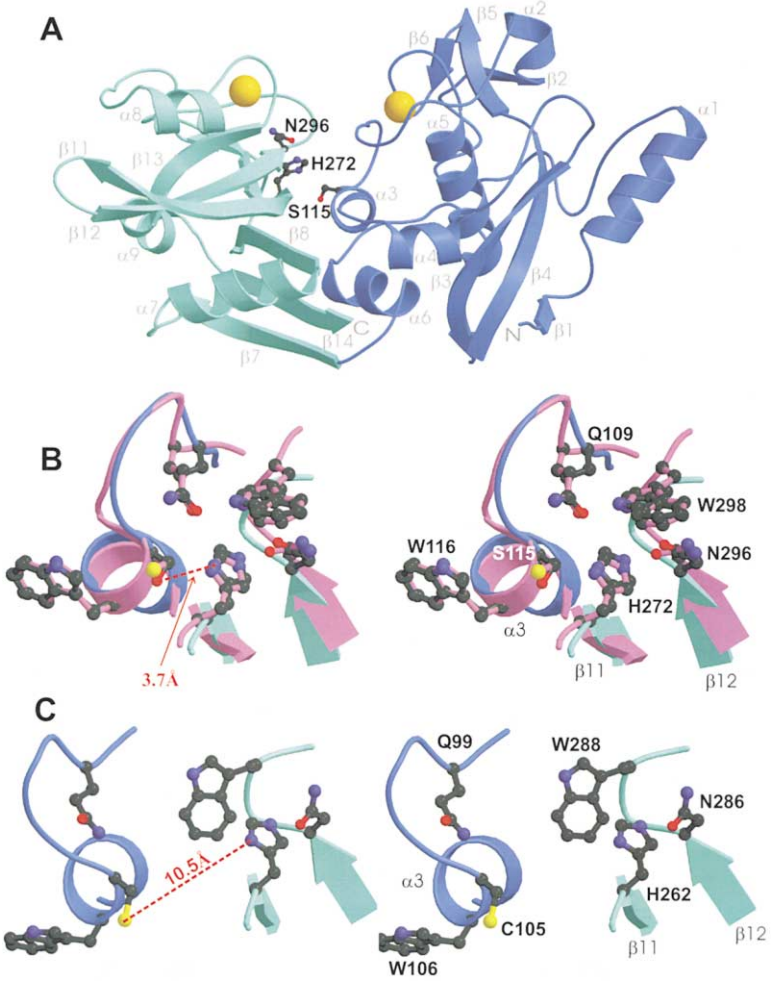

Figure 2. X-Ray Structure of Ca^{2+} Bound μI-II

(A) The front view of μI-II looking down α3 on which the active site cysteine resides is shown with DI colored in blue and DII in cyan. β strands and α helices are numbered sequentially from the N terminus (N) to the C terminus (C). Gold-colored spheres indicate the positions of the two Ca^{2+}. The side chain atoms of the catalytic triad residues are colored in red (oxygen), dark blue (nitrogen), and gray (carbon), and the bonds are colored in gray.

(B) Stereo view of the active site residue overlap between Ca^{2+} bound μI-II and papain. The side chains of active site residues in papain (PDB accession code 9PAP; Kamphuis et al., 1984; C25, H159, N175, Q19, W177, numbering not shown) were overlapped onto the side chains from corresponding residues in μI-II (S115, H272, N296, Q109, W298, numbers shown) using the program Lsqkab (Kabsch, 1976). The overlap of W116 is also included because this is a key residue in the hydrophobic core of DI. Papain secondary structure and side chain bonds are colored purple. Atoms and μI-II domains are colored as in (A) with the sulfur atom of the papain active site C25 colored yellow.

(C) Stereo view of the active site residues of Ca^{2+}-free human m calpain (Strobl et al., 2000).

Ca^{2+} ions appear to occupy surface-accessible positions between two peptide loops (Figure 3). The distance between the Ca^{2+} ions is ~17 Å. In addition, a new antiparallel β sheet is formed in DII between the short strands β9 and β10 (captioned in Figure 4G), which do not interact in the Ca^{2+}-free structure (Figure 4A).

Active Site Structure of the Ca^{2+} Bound μI-II Is Consistent with Enzyme Activity

The initial sequence analysis of calpain suggested a fusion of a papain-like cysteine protease with a calmodulin-like protein (Ohno et al., 1984). The structure of the inactive m calpain heterodimer reinforced this notion, and the Ca^{2+} bound μI-II structure extends this homology by defining the spacing between critical active site residues that are highly conserved among the various cysteine proteases, such as papain and the cathepsins (Berti and Storer, 1995). There is a striking similarity in location between the catalytic residues of Ca^{2+} bound μI-II and those of papain (Kamphuis et al., 1984). An overlap of the side chains of the catalytic triad residues S115, H272, and N296 in μI-II and of two closely associated residues, Q109 of the oxyanion hole and W298, onto the corresponding residues in papain (S25, H159, N175, Q19, W177) gave an overall rmsd for all side chain atoms of 0.66 Å (Figure 2B). Whereas the distance between the active site S105 O_γ and the imidazole N_δ of H262 of Ca^{2+}-free inactive m calpain is 10.5 Å (Figure 2C; Hosfield et al., 1999), this distance in the Ca^{2+} bound μI-II is 3.7 Å (Figure 2B), as it is in papain. The third residue of the charge relay system, N296, overlapped well with the corresponding residue of papain (N175). Moreover, the side chain amides of the oxyanion hole Q109 (μI-II) and of Q19 (papain) showed a perfect overlap in spite of differences in the positions of their C_α-C_β bond. W288 of inactive m calpain is positioned between DI and II, acting apparently as a wedge that prevents active site assembly (Figure 2C). In Ca^{2+} bound μI-II, the equivalent W298 is found retracted within DII in a similar position to that observed in papain (Figures 4F and 4G). The similarity of the active site residue orientations and spacings between μI-II and papain suggests that the catalytic mechanism of calpain is very similar if not identical to that of the Ca^{2+}-independent cysteine proteases.

Two Non-EF-Hand Ca^{2+} Binding Sites in the Cysteine Protease Region of Calpain

The μI-II structure in the presence of Ca^{2+} provides direct evidence for the existence of two non-EF-hand Ca^{2+} binding sites in the protease region of calpain. Each Ca^{2+} ion binds within a single domain. Two peptide

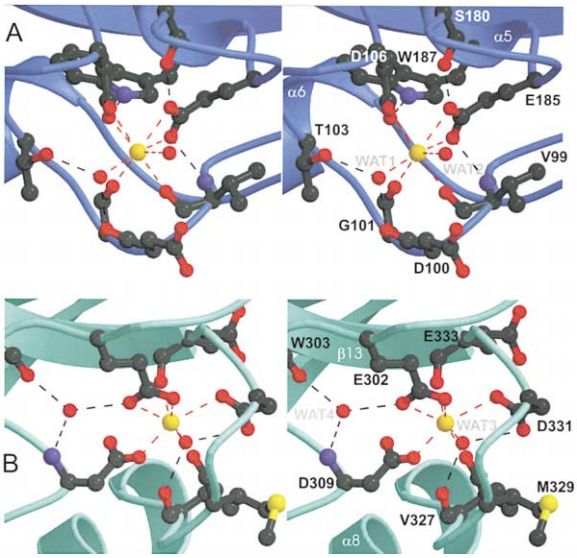

Figure 3. Two Novel Cooperative Ca^{2+} Binding Sites in the Protease Region of Calpain

(A) Ca^{2+}-coordination site in DI. Coordinations to Ca^{2+} (gold spheres) are shown by red dotted lines. Water molecules that coordinate Ca^{2+} are labeled WAT. Hydrogen bonds that stabilize the coordination complex are dotted black: N_ϵ of W187 to D106, S180 backbone oxygen and V99 backbone amide to E185, and T103 O_γ and D100 backbone oxygen to WAT1. The symmetrical arrangement of coordinations in DI should be noted: four of the equilateral coordinations are coplanar, drawing the vertices of a rectangle (E185, G101, WAT1), while the other four coordinations define a plane perpendicular to the first plane.

(B) DII Ca^{2+} site has pentagonal bipyramid geometry. Coloring is the same as in (A).

loops supply eight coordinations to the Ca^{2+} in DI (Figure 3A, red lines), in contrast to the pentagonal bipyramid configuration of most EF-hand motifs (Lewit-Bentley and Rety, 2000). Three residues on the loop preceding helix α3, which contains the active site C115, provide four coordinating oxygen atoms. The side chain of D106 offers two coordinations, while the backbone oxygens of V99 and G101 offer one each. Two other coordinations are provided by the side chain of E185, which is positioned on the loop leading to the N terminus of the core helix (α5). Two ordered water molecules donate the last two Ca^{2+} coordinations (Figure 3A, WAT1 and WAT2). Several hydrogen bonds stabilize the coordination complex (Figure 3A, black lines).

The Ca^{2+} binding site in DII exhibits pentagonal bipyramid coordination (Figure 3B). As in DI, two loops are involved in Ca^{2+} binding. The loop containing W298 makes two side chain coordinations (E302 and D309) to the Ca^{2+}. The loop conformation is additionally stabilized through an internal water molecule (WAT4) that bridges one O_ϵ of E302 to the carbonyl oxygen of W303 and to the backbone nitrogen of D309. From the second loop of the Ca^{2+} binding site in DII, another side chain coordination is made by D331, while backbone oxygens of E333 and M329 supply two other coordinations. The seventh coordination is provided by a water molecule (WAT3), which is stabilized by interactions with E331 O_δ and the backbone nitrogen of V327. The coordination distances in the two Ca^{2+} binding sites range from 2.04 Å (WAT3) to 2.90 Å (WAT2), with an average of 2.45 Å. These distances are similar to those observed in the well-studied Ca^{2+} binding EF-hand motifs of calmodulin (Babu et al., 1988).

Although the two Ca^{2+} binding sites are in separate domains, they are linked through a double salt bridge between the side chain of R104 (N_ϵ and N_η) and the side chain of E333 ($O_{\delta1}$ and $O_{\delta2}$; Figure 4D, black dotted lines). This interaction is very tight, with crystallographic B factors for R104 (20.4 $Å^2$) and E333 (23.1 $Å^2$) falling below the structure average of 27.3 $Å^2$ (Table 1), especially at the interacting atom positions. Since Ca^{2+}-coordinating residues in DI flank R104 and E333 directly coordinates Ca^{2+} in DII via its backbone oxygen, the R104/E333 interaction provides a structural basis for cooperativity between the two Ca^{2+} binding sites in calpain.

Ca^{2+}-Induced Conformational Changes in the Cysteine Protease Region of Calpain

The conformational changes induced by Ca^{2+} in the active site region (DI-II) are well illustrated by comparing the structure of the Ca^{2+}-free human m calpain heterodimer (Figure 4A; Strobl et al., 2000) to that of the Ca^{2+} bound μI-II (Figure 4G). At the level of the individual domains, changes in conformation occur mainly as peptide loop rearrangements (Figures 4B and 4E). The primary consequence of these intradomain conformational changes is the realignment of the two domains into the active conformation. DI of the m calpain heterodimer overlapped with DI of the Ca^{2+} bound μI-II with an overall C_α rmsd of 1.27 Å (Figure 4B). There is a close overlap for most of the secondary structure elements in DI (rmsd of ~1.0 Å). The differences originate mainly from the tightening of the large loop around the Ca^{2+} site, which has a C_α rmsd of ~5.0 Å for the residues found in the immediate vicinity of the Ca^{2+} (μ96–108). This loop contains R104 and three of the residues that coordinate Ca^{2+}, which are pulled closer toward DI. There is also a small movement of the associated helices (α2 and α3). Since the oxyanion hole residue Q109 and the active site residue C115 (C_α rmsd of 2.11 Å) reside on the loop and helix α3, respectively, DI Ca^{2+} binding influences their proper positioning in the active site. Interestingly, E185, which provides two coordinations to Ca^{2+} in DI, moves less because of the stabilization imposed by the core helix α5 (C_α rmsd of 1.55 Å). Nevertheless, its side chain is slightly rearranged upon Ca^{2+} binding.

The Ca^{2+}-induced conformational changes in DII are more pronounced than in DI (Figure 4E). As in DI, most of the secondary structure elements in DII overlap well with the Ca^{2+}-free form (C_α rmsd ~0.9 Å). Obvious differences occur in the region flanking strands β9 and β10 (residues 254–269, C_α rmsd of ~7.0 Å), which does not interact directly with Ca^{2+}. In the presence of Ca^{2+}, these strands come together to form a β sheet that provides supporting van der Waals contacts to the active site W298 through the side chain of the highly conserved V269. In μI-II, as in the m calpain heterodimer structure, this tryptophan (W288 in Figure 4A) presumably acts in the absence of Ca^{2+} as a wedge between the two domains. This residue probably contributes most to the overall change in fluorescence caused by Ca^{2+}. The two

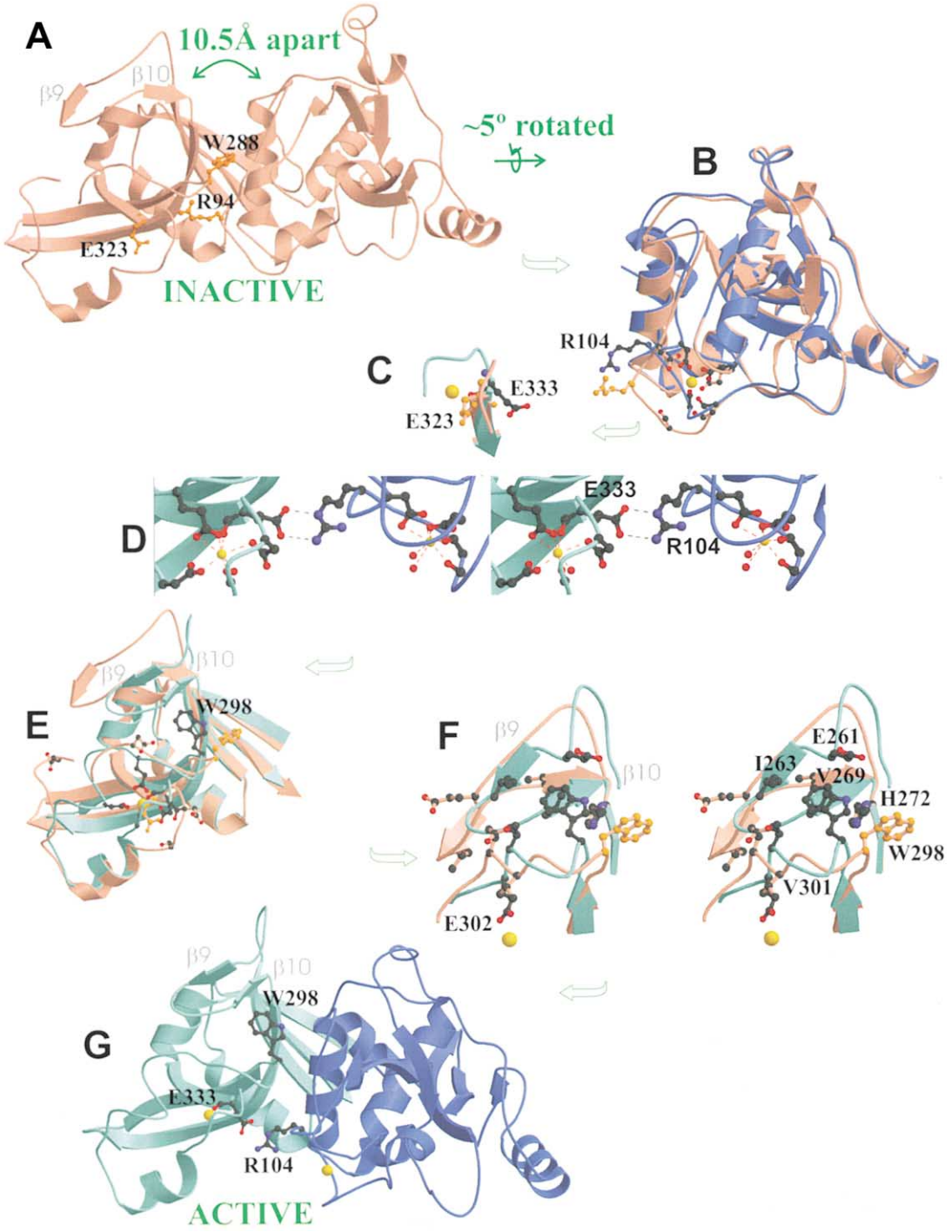

Figure 4. Ca^{2+}-Induced Conformational Changes in the Active Site Region of Calpain and Proposed Activation Mechanism

(A) DI and II of inactive human m calpain (Strobl et al., 2000). The ribbon presentation is colored pink, with the side chains of three critical residues (equivalent to μ R104, W298, and E333) colored orange. DI and II are rotated 5° relative to each other, and C105 and H262 are 10.5 Å apart.

(B) DI of μI-II (blue) was overlapped onto DI from m calpain (pink) using the program Align (Cohen, 1997). The gold sphere indicates the Ca^{2+} ion.

(C) Exposure of the Ca^{2+} binding site in DII (cyan) resulting from attraction of the E333 side chain by R104 from DI.

(D) R104-E333 double salt bridge stereo view.

(E) Overlap of DII from μI-II (cyan) onto DII from m calpain (pink) showing the loops that coordinate the second Ca^{2+}. Note: a discrepancy in the m calpain structure around G295 results in a discontinuity in that peptide loop.

(F) Stereo view of the hydrophobic pocket formed by Ca^{2+} binding to DII.

(G) Ca^{2+} bound μI-II, showing the arrangement of the Ca^{2+} ions relative to the active site cleft. This is a 90° rotation of the view in Figure 2A.

Table 1. Crystallographic Data

Data Collection Statistics	Total	Outer Shell
Resolution range (Å)	30.00–2.07	2.14–2.07
Measured reflections	119,331	18,655
Unique reflections	43,051	4,388
Completeness (%)	92.0	94.6
I/σI	11.3	2.8
R_{merge}[a] (%)	9.1 (14.0)	39.0 (36.8)
Refined Structural Model		
Free reflections (5% of unique)	2,154	
R_{cryst}[b] (%)	21.8	
R_{free} (%)	25.7	
No. of protein/solvent/Ca^{2+} atoms (excl. H)	5147/255/4	
Bond angle rmsd (°)	1.232	
Bond length rmsd (Å)	0.006	
Average Bfactor (Å^2)	27.3	

The unit cell dimensions were $a = 149.4$ Å, $b = 40.49$ Å, $c = 132.3$ Å and $\beta = 106.0°$. The two molecules in the asymmetric unit overlapped with rmsd of 0.23 Å.

[a] $R_{merge} = \Sigma|I_j - \langle I\rangle|/\Sigma I_j$, where I_j are individual measurements for any on reflection and $\langle I\rangle$ is the average intensity of the symmetry equivalent reflections.

[b] $R_{cryst} = \Sigma|F_o - F_c|/\Sigma F_o$, F_o and F_c are observed and calculated structure factor amplitudes, respectively.

loops that contain the Ca^{2+}-coordinating residues along with helix α8, which is flanked by them, undergo a marked conformational change (residues 302–310 and 328–333, C_α rmsd of ~3.0 Å). In contrast, the two residues of the catalytic triad that reside in DII (H272 0.20 Å, N296 0.96 Å) show low C_α rmsd in the overlap.

Structural Insights into the Ca^{2+}-Dependent Activation Mechanism in the Protease Region of Calpain

Detailed examination of the Ca^{2+} binding sites and the Ca^{2+}-induced conformational changes allows us to postulate a structural mechanism of μI-II activation (Figure 4). We propose that the Ca^{2+}-coordinating residue E185, which moves very little upon Ca^{2+} binding, acts as the nucleation site (Figures 3A and 4B) and that Ca^{2+} binds first at this partially "preformed" site in DI. A preformed Ca^{2+} site observed in the N-terminal domain of troponin C (N-TnC site II) has been shown to have a higher affinity for Ca^{2+} than site I of N-TnC, as it requires less energy to rearrange the Ca^{2+}-coordinating elements for ligand binding (Strynadka et al., 1997). The other three coordinating residues in DI belong to a flexible loop (μ96–108). The movement of this loop appears to be the only significant energetic barrier that Ca^{2+} binding has to overcome in DI. As this loop adopts the Ca^{2+} bound conformation, R104, which in the inactive heterodimer is surface exposed, is brought around the 328–332 loop of DII and positioned at a less surface-accessible site to interact with the side chain of E333 (Figures 4C and 4D).

None of the Ca^{2+}-coordinating residues in DII provide an already existing nucleation site for Ca^{2+} binding (Figure 4E). Moreover, the energetic barrier is presumably larger than in DI, as two loops, rather than one, have to undergo major rearrangement, and the Ca^{2+}-coordinating residues must move farther than in DI. Furthermore, the side chain of E333 in the absence of Ca^{2+} (orange, Figure 4C) provides a steric barrier to Ca^{2+} binding, because it overlaps the Ca^{2+} position. The requisite peptide backbone rotation at residue E333 in the presence of Ca^{2+} is likely to be the initial event that exposes the first Ca^{2+}-coordinating residue in DII. We suggest that the electropositive environment contributed by the repositioned R104 side chain attracts the electronegative side chain of E333 and is the energetic trigger for the rotation. Once exposed, the carbonyl oxygen of E333 acts as a nucleation site for Ca^{2+} binding, leading to recruitment of the other Ca^{2+}-coordinating residues.

A further critical event is the displacement of W298 from its position between the two domains. This is influenced by the side chain rearrangement of the neighboring residue E302 as it moves toward the Ca^{2+}, making room for the short Ca^{2+}-induced antiparallel sheet β9-β10 to form at an adjacent site and provide stabilizing van der Waals interactions to W298 (Figure 4F). Two conserved valine residues, V269 and V301, together with I263 form a hydrophobic pocket that interacts with the nonpolar region of the indole ring of W298, while the highly conserved E261 side chain hydrogen bonds to N_ϵ of W298. Removal of the W298 side chain from its position between the two domains is a key step in permitting the two domains to come together and assume the catalytically competent papain-like arrangement of the key active site residues (Figure 2B).

Residues Involved in the Ca^{2+} Switch Mechanism Are Highly Conserved

We have aligned the amino acid sequences of rat μI-II with representative isoforms from the calpain superfamily to see if the structural determinants for Ca^{2+}-dependence in the protease region are conserved. The aligned isoforms have identical residues at all five side chain-dependent Ca^{2+}-coordinating positions (Figure 5). Some of the residues that provide backbone carbonyl Ca^{2+} coordinations are also highly conserved, as illustrated by G101. This glycine potentially confers flexibility to the Ca^{2+} binding loop (residues 96–108, top, pink bar). E333 and R104, which presumably interact as in μI-II to form the double salt bridge between the two Ca^{2+} binding sites, are present in all the displayed isoforms except *C. elegans* tra3 (Figure 5, blue highlights).

Discussion

The major discovery of this study is that Ca^{2+} binds cooperatively to two non-EF-hand sites in the protease core, DI and II, of μ calpain. Binding at these regulatory sites aligns the active site cleft and converts the core into an active enzyme with calpain-like specificity. One reason why the protease core is less active than wild-type μ calpain at submillimolar $CaCl_2$ concentrations could be the loss of structural support from neighboring domains, particularly DIII. In the absence of the domain contacts that occur within the wild-type calpain environment, the activity of the protease core can be partially restored by divalent cations (and to a lesser extent by NaCl), which might help compensate for missing salt linkages and induce tightening of the exposed hydrophobic patches at the lost interface. It is perhaps

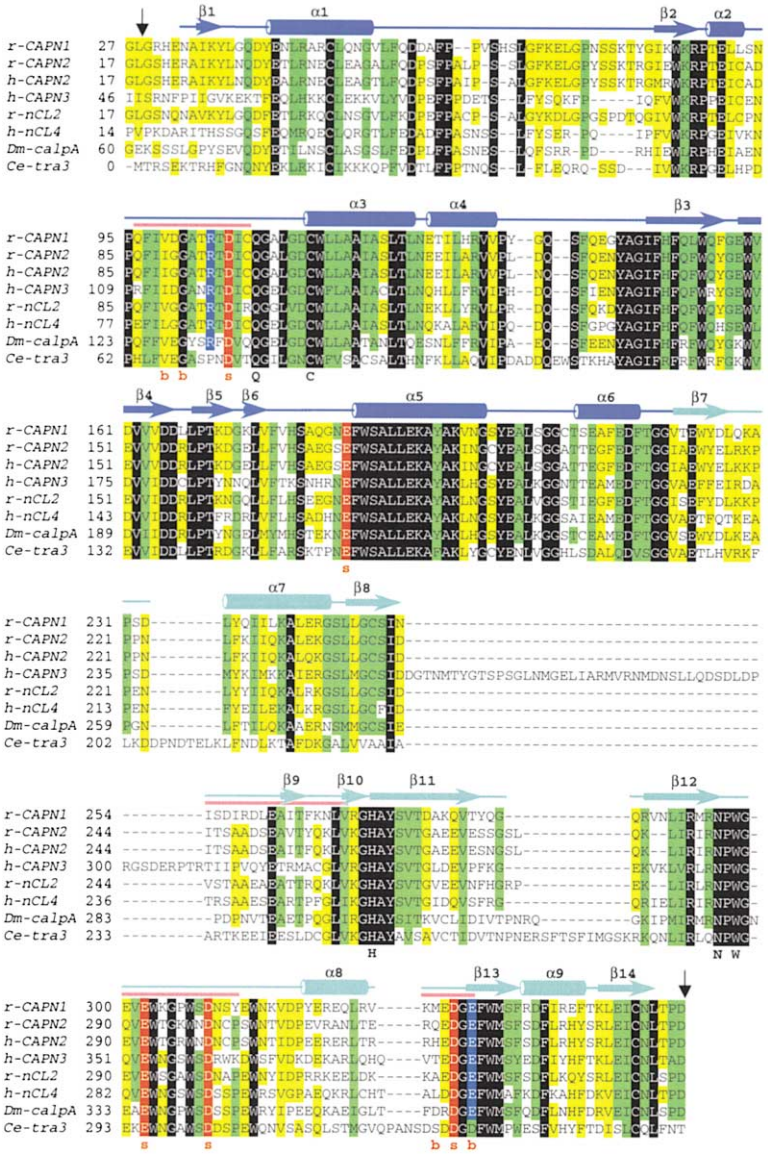

Figure 5. Conservation of Ca^{2+} Binding Determinants in Calpain Large Subunit Homologs

The sequence of the protease region (μI-II) of rat μ calpain (r-CAPN1; delimited by black arrows) was aligned using clustalW (Thompson et al., 1994), with the corresponding region from seven isoforms, rat m calpain (r-CAPN2), human m calpain (h-CAPN2), human p94 (h-CAPN3), rat nCL2 (r-nCL2), human nCL4 (h-nCL4), *Drosophila melanogaster* calpA (Dm-calpA), and *Caenorhabditis elegans* tra3 (Ce-tra3). Accession numbers for these isoforms are NP_062025.1, AAA16327.1, A31218, A56218, A48764, XP_001445.1, CAA55297.1, and S71885, respectively. The identity level between isoforms is indicated in black (100%), green (≥75%), and yellow (≥50%). Residues that coordinate Ca^{2+} through their side chain are highlighted in red with a red "s" below the alignment. Backbone coordinations are marked with a red "b" below the alignment. Conservation of R104 and E333 is indicated by blue highlights. Catalytic residues are shown in bold below the alignment. Above the alignment the secondary structure elements are shown with the sheets and helices numbered and colored as in Figure 2. The pink bars correspond to regions that have a different conformation in the inactive human m calpain heterodimer as seen in Figure 4.

significant that μI-II crystals were only formed in the presence of 1.5 M NaCl and 10 mM $CaCl_2$.

The proposed structure-based activation mechanism of the protease core of μ calpain by Ca^{2+} occurs in the following sequence: Ca^{2+} binding at a partially preformed site in DI repositions the R104 side chain which, via a double salt link interaction with the side chain of E333 in DII, triggers a rotation of the peptide backbone that contains E333. The exposure of the first Ca^{2+}-coordinating oxygen (E333's backbone oxygen) in the second Ca^{2+} site is followed by Ca^{2+}-induced conformational changes in DII that allow the formation of a hydrophobic pocket to accommodate W298's side chain. This side chain swings away from the cleft into the pocket, thereby allowing the realignment of the two domains in the active conformation. These conformational changes define a novel Ca^{2+} binding mechanism that leads to activation of these Ca^{2+} signaling proteases, which then precisely cleave specific downstream targets in a variety of signaling pathways, in turn modulating their activities.

We propose that the wild-type μ and m calpains undergo a Ca^{2+}-dependent two-stage activation (Figure 6). Stage 1 is the release of constraints imposed by the circular arrangement of domains. This involves subtle conformational changes in DIV and VI that lead to dissociation of the large subunit N-terminal anchor peptide (red helix in Figure 6) from the small subunit DVI (Nakagawa et al., 2001), conformational changes in DIII (Hosfield et al., 2001), and perhaps small subunit dissociation (Yoshizawa et al., 1995; Pal et al., 2001). The anchor peptide is cleaved during autolysis, thus significantly lowering the Ca^{2+} requirement of the heterodimeric calpains. Stage 2 is the realignment of the active site cleft caused by the cooperative binding of Ca^{2+} to DI and II. Release of constraints is a precondition of activation, so that stage 2 cannot take place before stage 1. This was shown by mutations that reduced the Ca^{2+} binding affinity at one or more EF-hands in one or both of DIV and VI (Dutt et al., 2000). As Ca^{2+} binding at one or more EF hands in the large and small subunits was reduced

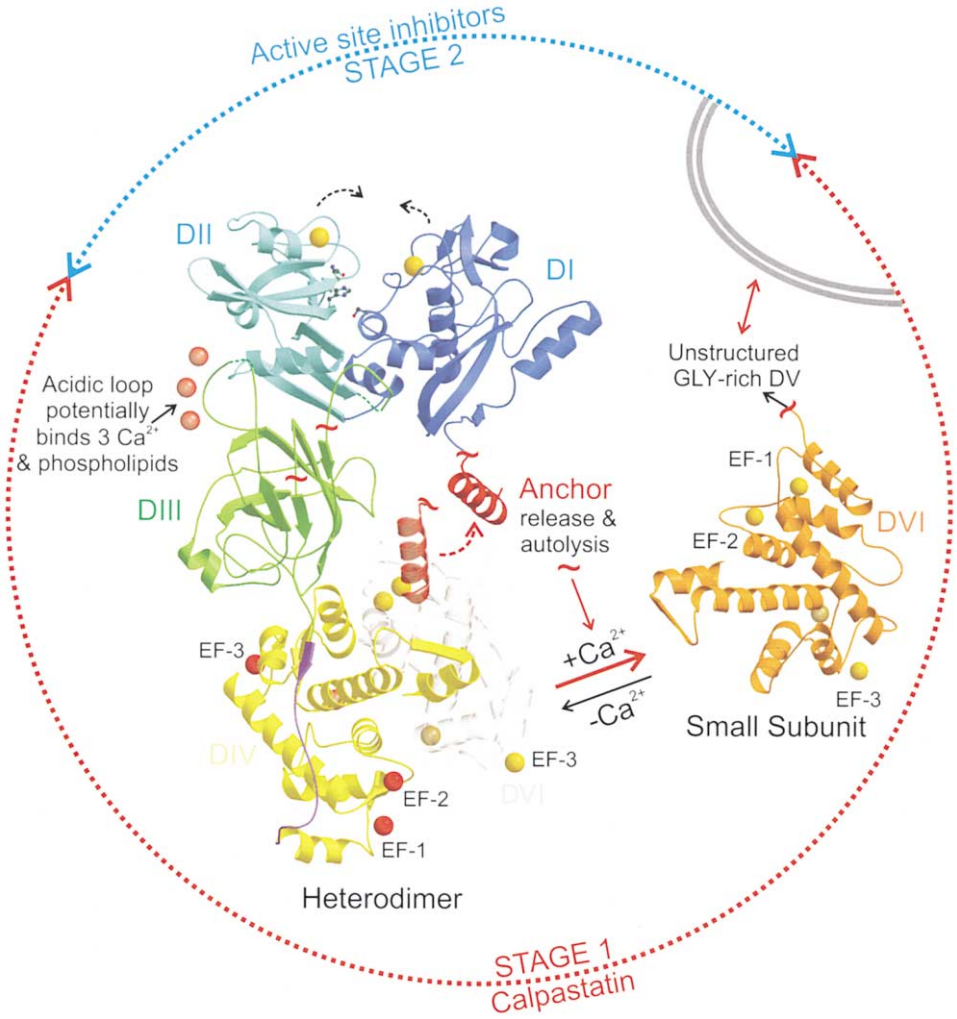

Figure 6. Regulation of Heterodimeric Calpain by Ca^{2+}

A generic model for Ca^{2+} bound calpain was constructed by substituting the Ca^{2+} bound structure of DI-II into the human m calpain heterodimer (Strobl et al., 2000) while overlapping DIV and VI with the Ca^{2+} bound DVI heterodimer structure (Blanchard et al., 1997). DII was positioned to optimize DIII interactions. The anchor peptide (red helix) was placed in the Ca^{2+}-free conformation where it interacts with DVI (gray). Two consecutive yet cooperative levels of Ca^{2+} regulation are proposed, both acting on a different segment of the circularized structure. Stage 1 includes anchor release (Nakagawa et al., 2001), shown by the red dotted arrow. As well, under certain conditions small subunit dissociation (Pal et al., 2001) and the potential binding of Ca^{2+} to DIII (Hosfield et al., 2001; Tompa et al. 2001) may help free the protease region from constraints. Stage 2 is active site assembly (black dotted arrows) as seen in μI-II. It follows the onset of stage 1 but may also influence it if the tendency to realign the active site pulls against the restraint. Ca^{2+} ions are colored gold (seen in X-ray structures) or red (postulated or confirmed by mutagenesis; Dutt et al., 2000). Transparent spheres in DIV and VI are Ca^{2+} at EF-4 sites that are likely filled only at high $CaCl_2$ (>20 mM) concentrations. Calpain association with membranes (double gray lines) may also contribute to activation (as reviewed in Nakagawa et al., 2001).

or abolished, higher concentrations of Ca^{2+} were required for activation. Nevertheless, stage 2 seems to influence stage 1, as the μ/m chimera (in which the core of m calpain is replaced by the μ calpain core) has a significantly lower Ca^{2+}-requirement (~120 μM) than wild-type m calpain (~340 μM), yet a much higher one than that of the μ calpain core alone (~40 μM $CaCl_2$). Since the interactions between the anchor peptide and DVI as well as those between DIV and DVI are identical in the μ/m chimera and the wild-type m calpain, interactions of the protease core (DI-II) with DIII must account for the observed differences in Ca^{2+} requirement, suggesting that these interactions directly affect the realignment of the protease core. Thus, the anchor and the domains outside of the protease core add an extra level of Ca^{2+} regulation that keeps the active site from being assembled in heterodimeric calpains.

The endogenous calpain inhibitor calpastatin contains four equivalent domains, each possessing similar inhibitory activity against calpain (Maki et al., 1991). Within each domain there are three segments (A, B, and C) that can independently bind to different domains of calpain. Segment C binds DVI and segment A binds DIV, while segment B binds to an as yet unidentified site likely residing close to the active site or within DIII. In isolation only segment B possesses calpain-inhibitory activity.

μI-II was not inhibited by domain I of calpastatin or by a peptide corresponding to segment B (T.M., unpublished data), suggesting that calpastatin does not bind at the active site of calpain. Since DIII-VI mediate the physiological regulation of calpain by calpastatin (Figure 6), calpain isoforms that lack these domains might also escape inhibition by calpastatin. It is interesting that calpastatin and the heterodimeric calpains are both found only in mammals, suggesting the two may have evolved in concert to extend the physiological regulation of a progenitor Ca^{2+}-dependent cysteine protease.

The heterodimeric calpains are remarkable enzymes for their number and variety of Ca^{2+} binding sites (Figure 6). There are at least three different types of Ca^{2+} sites (EF-hand, C2-like domain, and protease domain sites) that act in concert to regulate the biological function of the enzyme. There are potentially up to six Ca^{2+} bound to DIV + VI, apparently at EF-hands 2 and 3, and possibly at unconventional EF-hand 1 (Blanchard et al., 1997; Lin et al., 1997; Dutt et al., 2000). It has been reported that recombinant C2-like DIII from m calpain binds Ca^{2+}, presumably to the cluster of acidic residues on exposed surface loops that in m calpain lie adjacent to DII (Tompa et al., 2001). C2 domains can potentially bind up to three Ca^{2+} (Rizo and Sudhof, 1998). In this study we have discovered two Ca^{2+} binding sites in DI and II that do not have obvious equivalents in other proteins. These two sites each have Ca^{2+}-coordinating residues derived from two peptide loops that appear to have been added in an evolutionary sense onto a papain-like precursor protease. This unsuspected role for Ca^{2+} helps to rationalize the extensive literature showing that heterodimeric calpains retain a Ca^{2+} requirement for hydrolysis of substrates that is lower than that required for the initial activation step.

The two active site domains are present in all members of the calpain superfamily, whereas the flanking domains are varied (Sorimachi and Suzuki, 2001). Thus, the cooperative binding of Ca^{2+} to DI and II demonstrates a new role of Ca^{2+} as a second messenger, which has wide implications in calpain signaling. It suggests a general Ca^{2+} activation mechanism for calpain superfamily members including those that do not contain the small subunit and those that lack EF-hand or C2-like domains in the large subunit. Accordingly, some of the nonheterodimeric calpains might bypass the first activation barrier and could be directly activated by the second mechanism. Alignments of DI and II illustrate the conservation of the Ca^{2+}-chelating side chains in calpain isoforms in numerous organisms ranging from mammals to bacteria. For example, our alignment suggests that the muscle-specific calpain isoform p94, which is linked to limb girdle muscular dystrophy 2A (Richard et al., 1995), could be governed by a similar mechanism of activation by Ca^{2+} in the protease region (Branca et al., 1999). This isoform lacks the small subunit but has a domain structure similar to that of the large subunit of the heterodimeric calpains. Moreover, in many of these calpains, such as the p94 isoform, the E333 and R104 residues that form the double salt bridge pair between the two Ca^{2+} binding sites are also conserved. It appears that this Ca^{2+} activation mechanism is ancient and that additional constraints on activation have been added subsequently as in the μ and m calpains.

Another important aspect relevant to the pathophysiological roles of calpain based on the properties of μI-II is the possibility that the natural autolytic cleavage product (DI, II, and part of III) might remain active in vivo for some considerable time after autolysis. We have observed that μI-II is resistant to autoproteolysis for many hours in the presence of Ca^{2+} (data not shown) and that it is not inhibited by calpastatin. In this way, the natural fragment may escape the regulation imposed on the holoenzyme. Thus, residual calpain activity could remain after autolysis, which has implications for the inhibition of pathologies, suggesting a continual need for administration of calpain inhibitors throughout the duration of ischemic episodes. Fortunately, the structural information contained here together with the stability and ease of preparation of μI-II should facilitate the design and testing of inhibitors for the calpains.

Experimental Procedures

Cloning of the Protease Region from Rat μ Calpain and Its Swap into m Calpain

The μI-II construct extends from the second calpain autolysis site, residue 29 (MG^{29}RHENA→), which defines the start of DI, to the end of DII (residue 356). This region was PCR amplified from rat μ calpain large subunit DNA using Pfu DNA polymerase (Clontech) and cloned into pET24d vector (Novagen) to include the C-terminal hexahistidine tag (→$NLTPD^{356}$KLAAALEH_6). To perform fluorescence measurements and crystallization in the presence of Ca^{2+} without the risk of proteolysis, the active site Cys was mutated to Ser by the single-stranded DNA method (Kunkel et al., 1991). The μ/m calpain hybrid was made by replacing large subunit residues 19–346 from recombinant rat m calpain (Elce et al., 1995) with residues 29–356 of rat μ calpain (T.M., unpublished data).

Protein Expression and Purification

μI-II was expressed in *E. coli* BL21 (DE3) under kanamycin selection. The μ/m hybrid large subunit was coexpressed with the 21 kDa truncated small subunit under both kanamycin and ampicillin selection as previously described for m calpain (Elce et al., 1995). *E. coli* were grown in 4 l LB broth (Fisher) at 37°C, and protein expression was induced with 0.4 mM isopropyl-1-thio-β-D-galactopyranoside after decreasing the temperature to 20°C. Calpains were purified over four columns as previously described (Elce et al., 1995), but with Sephadex G-75 substituting for Sephacryl S-200 in the case of μI-II. They were detected in the DEAE column eluate by immunoblotting using an anti-His-tag antibody (Clontech), and in other column profiles by SDS-PAGE. After the final purification step, μI-II was concentrated to ~50 mg/ml in storage buffer (10 mM HEPES [pH 7.6], 10 mM DTT) in a Biomax 10K concentrator (Millipore). Aliquots (50 μl) were flash-frozen in liquid nitrogen and stored at −70°C. A 4 l preparation yielded 10–40 mg of μI-II and ~5 mg of μ/m calpain.

Crystallization and Structure Determination

Crystallization of the C115S μI-II construct in the presence of Ca^{2+} was performed by the hanging drop vapor diffusion method with the well solution containing 1.5 M NaCl, 2% PEG 6000, 0.1 M MES (pH 6.0), 15% glycerol, and 10 mM $CaCl_2$. The drop size was less than 5 μl and contained an equal volume of well solution and protein solution. Prior to addition to the drop, the protein concentration was 12.5 mg/ml. Crystals grew in a few days, and prior to data collection they were cryoprotected by serial soakings (each for up to 5 min) in stabilization solutions containing 20%, 25%, and 30% (v/v) glycerol. Diffraction data were collected on a home source with a Rigaku rotating anode, a Mar300 detector, and an Oxford cryosystem using 0.5° oscillations and were processed (Table 1) using the HKL program suite (Otwinowski and Minor, 1997) and the CCP4 program suit (Collaborative Computational Project, 1994). The space group was C_2 with two molecules per asymmetric unit (Table 1). The struc-

ture was determined by molecular replacement using AMoRe (Navaza, 1994) with the structure of the Ca^{2+}-free rat m calpain DI and II (Hosfield et al., 1999) as a model. Most of the DI and II model fit the μI-II electron density map well, with the dissimilar regions being manually traced in XFIT (McRee, 1992). Refinement was performed using the CNS package (Brünger, 1998). PROCHECK (Laskowski et al., 1993) was used to assess the quality of the model with >87% of the residues lying in the most favorable regions of the Ramachandran plot and no residues in the disallowed regions. All structure diagrams were generated using Molscript (Kraulis, 1991) and RASTER3D (Merritt and Bacon, 1997).

Activity of μI-II against Protein and Synthetic Peptide Substrates

Proteolysis of the C105S m calpain heterodimer was performed at 22°C in a final volume of less than 150 μl, in 50 mM HEPES (pH 7.6), 1 mg/ml (10 μM) calpain, 0.015 mg/ml (0.4 μM) μI-II, without divalent cations, or with 1 mM $CaCl_2$ or 1 mM $MgCl_2$. Control reactions lacked μI-II or contained EDTA instead of $CaCl_2$. At specific time intervals, aliquots were removed, reaction was stopped by the addition of 2 × SDS gel sample buffer, and the results were analyzed by SDS-PAGE using a 9% gel.

The activity of 2.5 μM μI-II against the peptide substrate succinyl-leucine-tyrosine-aminomethyl coumarin (SLY-MCA; Sigma) was assayed in 50 mM HEPES (pH 7.6), 200 mM NaCl, 1 mM DTT, 0.5–30 mM divalent cation ($CaCl_2$, $MgCl_2$, $MnCl_2$, or $ZnCl_2$), 0.38 mM SLY-MCA, in a final volume of 3 ml. The effects of increasing concentrations of $CaCl_2$ (up to 100 mM) and of $MgCl_2$ (up to 200 mM) or NaCl (up to 400 mM) in the presence of 1.0 mM $CaCl_2$ were also tested. MCA release was monitored in a LS50B Perkin Elmer fluorescence spectrometer set with excitation and emission wavelengths at 360 nm and 460 nm, respectively. Steady-state kinetic analysis was performed under the same buffer conditions but in the presence of 0.5, 5, or 20 mM $CaCl_2$, varying SLY-MCA concentration from 0.01–1.0 mM. The steady-state parameters (k_{cat} and K_M) were obtained from the Michaelis-Menten plot. SLY-MCA hydrolysis by 15 nM μ/m calpain was analyzed under the same reaction conditions as for μI-II. Titrations of 2.5 μM μI-II, 15 nM μ/m calpain or m80k/21k with $CaCl_2$ were performed by varying $CaCl_2$ concentrations from 0.007 to 1.0 mM.

Intrinsic Tryptophan Fluorescence Measurements of μI-II

Intrinsic tryptophan fluorescence measurements were performed in a Perkin Elmer LS50B fluorescence spectrophotometer at 22°C using a stirrer-adapted 4 ml cuvette (Helma). Excitation and emission wavelengths were set at 280 nm and 340 nm, respectively. The reaction buffer was the same as that used for activity measurements against SLY-MCA, and the protein concentration was 0.65 μM. To avoid autolysis, the inactive C115S μI-II was used. $CaCl_2$ (50 mM) dissolved in the reaction buffer was continuously pumped (4 μl/min, Harvard Apparatus pump 22) through a tube into the cuvette using a 250 μl microsyringe (Hamilton-microliter 1000 series gastight). The reaction solution was vigorously mixed using the internal magnetic stirrer of the fluorimeter. The fluorescence intensity was corrected for dilution, and the normalized data were fitted to the Hill equation $y = x^n/(k^n + x^n)$, where y is the fraction of maximum intensity change, $k = [Ca^{2+}]_{0.5}$ (the value of $[Ca^{2+}]$ at which half-maximum intensity change is observed), n is the Hill coefficient, and x is $[Ca^{2+}]$. Intrinsic tryptophan fluorescence measurements were also performed under the same buffer conditions but with $MgCl_2$, $MnCl_2$, or $ZnCl_2$ up to 30 mM in place of $CaCl_2$. No significant aggregation was detected by light scattering even at the highest $CaCl_2$ concentration (30 mM) tested.

Acknowledgments

This work was funded by the Government of Canada's Network of Centres of Excellence program supported by the Canadian Institutes of Health Research and the Natural Sciences and Engineering Research Council through PENCE (the Protein Engineering Network of Centres of Excellence). P.L.D. is a Killam Research Fellow and T.M. is supported by an Ontario Graduate Scholarship.

Received: August 2, 2001
Revised: January 18, 2002

References

Arthur, J.S., Elce, J.S., Hegadorn, C., Williams, K., and Greer, P.A. (2000). Disruption of the murine calpain small subunit gene, Capn4: calpain is essential for embryonic development but not for cell growth and division. Mol. Cell. Biol. *20*, 4474–4481.

Babu, Y.S., Bugg, C.E., and Cook, W.J. (1988). Structure of calmodulin refined at 2.2 Å resolution. J. Mol. Biol. *204*, 191–204.

Benetti, R., Del Sal, G., Monte, M., Paroni, G., Brancolini, C., and Schneider, C. (2001). The death substrate Gas2 binds m calpain and increases susceptibility to p53-dependent apoptosis. EMBO J. *20*, 2702–2714.

Berti, P.J., and Storer, A.C. (1995). Alignment/phylogeny of the papain superfamily of cysteine proteases. J. Mol. Biol. *246*, 273–283.

Blanchard, H., Grochulski, P., Li, Y., Arthur, J.S., Davies, P.L., Elce, J.S., and Cygler, M. (1997). Structure of a calpain Ca^{2+}-binding domain reveals a novel EF-hand and Ca^{2+}-induced conformational changes. Nat. Struct. Biol. *4*, 532–538.

Branca, D., Gugliucci, A., Bano, D., Brini, M., and Carafoli, E. (1999). Expression, partial purification and functional properties of the muscle-specific calpain isoform p94. Eur. J. Biochem. *265*, 839–846.

Brünger, A.T. (1998). Crystallography and NMR system: a new software system for macromolecular structure determination. Acta Crystallogr. *D45*, 905–921.

Carafoli, E., and Molinari, M. (1998). Calpain: a protease in search of a function? Biochem. Biophys. Res. Commun. *247*, 193–203.

Carragher, N.O., Westhoff, M.A., Riley, D., Potter, D.A., Dutt, P., Elce, J.S., Greer, P.A., and Frame, M.C. (2002). v-Src-induced modulation of the calpain-calpastatin proteolytic system regulates transformation. Mol. Cell. Biol. *22*, 257–269.

CCP4 (Collaborative Computational Project 4) (1994). The CCP4 suite: progams for protein crystallography. Acta Crystallogr. D *50*, 760–763.

Cohen, G.E. (1997). ALIGN: a program to superimpose protein coordinates, accounting for insertions and deletions. J. Appl. Crystallogr. *30*, 1160–1161.

Cox, E.A., and Huttenlocher, A. (1998). Regulation of integrin-mediated adhesion during cell migration. Microsc. Res. Tech. *43*, 412–419.

Crawford, C., Brown, N.R., and Willis, A.C. (1993). Studies of the active site of m calpain and the interaction with calpastatin. Biochem. J. *296*, 135–142.

Croall, D.E., and DeMartino, G.N. (1991). Calcium-activated neutral protease (calpain) system: structure, function, and regulation. Physiol. Rev. *71*, 813–847.

Dourdin, N., Bhatt, A.K., Dutt, P., Greer, P.A., Arthur, J.S., Elce, J.S., and Huttenlocher, A. (2001). Reduced cell migration and disruption of the actin cytoskeleton in calpain-deficient embyonic fibroblasts. J. Biol. Chem. *276*, 48382–48388.

Dutt, P., Arthur, J.S., Grochulski, P., Cygler, M., and Elce, J.S. (2000). Roles of individual EF-hands in the activation of m calpain by calcium. Biochem. J. *348*, 37–43.

Elce, J.S., Hegadorn, C., Gauthier, S., Vince, J.W., and Davies, P.L. (1995). Recombinant calpain II: improved expression systems and production of a C105A active-site mutant for crystallography. Protein Eng. *8*, 843–848.

Glading, A., Lauffenburger, D.A., and Wells, A. (2002). Cutting to the chase: calpain proteases in cell motility. Trends Cell Biol. *12*, 46–54.

Hosfield, C.M., Elce, J.S., Davies, P.L., and Jia, Z. (1999). Crystal structure of calpain reveals the structural basis for Ca^{2+}-dependent protease activity and a novel mode of enzyme activation. EMBO J. *18*, 6880–6889.

Hosfield, C.M., Moldoveanu, T., Davies, P.L., Elce, J.S., and Jia, Z. (2001). Calpain mutants with increased Ca^{2+} sensitivity and implications for the role of the C_2-like domain. J. Biol. Chem. *276*, 7404–7407.

Kabsch, W. (1976). A solution for the best rotation to relate two sets of vectors. Acta Crystallogr. *A32*, 922–923.

Kamphuis, I.G., Kalk, K.H., Swarte, M.B., and Drenth, J. (1984). Structure of papain refined at 1.65 Å resolution. J. Mol. Biol. *179*, 233–256.

Kraulis, P.J. (1991). MOLSCRIPT: a program to produce both detailed and schematic plots of protein structures. J. Appl. Crystallogr. *24*, 946–950.

Kunkel, T.A., Bebenek, K., and McClary, J. (1991). Efficient site-directed mutagenesis using uracil-containing DNA. Methods Enzymol. *204*, 125–139.

Laskowski, R.A., MacArthur, M.W., Moss, D.S., and Thornton, J.M. (1993). PROCHECK: a program to check the stereochemical quality of protein structures. J. Appl. Crystallogr. *26*, 283–291.

Lee, K.S., Yanamoto, H., Fergus, A., Hong, S.C., Kang, S.D., Cappelletto, B., Toyoda, T., Kassell, N.F., Bavbek, M., and Kwan, A.L. (1997). Calcium-activated proteolysis as a therapeutic target in cerebrovascular disease. Ann. N Y Acad. Sci. *825*, 95–103.

Lee, M.S., Kwon, Y.T., Li, M., Peng, J., Friedlander, R.M., and Tsai, L.H. (2000). Neurotoxicity induces cleavage of p35 to p25 by calpain. Nature *405*, 360–364.

Lewit-Bentley, A., and Rety, S. (2000). EF-hand calcium-binding proteins. Curr. Opin. Struct. Biol. *10*, 637–643.

Lin, G.D., Chattopadhyay, D., Maki, M., Wang, K.K., Carson, M., Jin, L., Yuen, P.W., Takano, E., Hatanaka, M., DeLucas, L.J., and Narayana, S.G. (1997). Crystal structure of calcium bound domain VI of calpain at 1.9 Å resolution and its role in enzyme assembly, regulation, and inhibitor binding. Nat. Struct. Biol. *4*, 539–547.

Maki, M., Ma, H., Takano, E., Adachi, Y., Lee, W.J., Hatanaka, M., and Murachi, T. (1991). Calpastatins: biochemical and molecular biological studies. Biomed. Biochim. Acta *50*, 509–516.

McRee, D.E. (1992). A visual protein crystallographic software system for X11/XView. J. Mol. Graph. *10*, 44–46.

Merritt, E.A., and Bacon, D.J. (1997). RASTER3D: photorealistic molecular graphics. Methods Enzymol. *277*, 505–524.

Nakagawa, K., Masumoto, H., Sorimachi, H., and Suzuki, K. (2001). Dissociation of m calpain subunits occurs after autolysis of the N-terminus of the catalytic subunit, and is not required for activation. J. Biochem. *130*, 605–611.

Navaza, J. (1994). AMoRe: an automated package for molecular replacement. Acta Crystallogr. *A50*, 157–163.

Nishimura, T., and Goll, D.E. (1991). Binding of calpain fragments to calpastatin. J. Biol. Chem. *266*, 11842–11850.

Nixon, R.A. (2000). A "protease activation cascade" in the pathogenesis of Alzheimer's disease. Ann. N Y Acad. Sci. *924*, 117–131.

Ohno, S., Emori, Y., Imajoh, S., Kawasaki, H., Kisaragi, M., and Suzuki, K. (1984). Evolutionary origin of a calcium-dependent protease by fusion of genes for a thiol protease and a calcium-binding protein? Nature *312*, 566–570.

Ono, Y., Shimada, H., Sorimachi, H., Richard, I., Saido, T.C., Beckmann, J.S., Ishiura, S., and Suzuki, K. (1998). Functional defects of a muscle-specific calpain, p94, caused by mutations associated with limb-girdle muscular dystrophy type 2A. J. Biol. Chem. *273*, 17073–17078.

Otwinowski, Z., and Minor, W. (1997). Processing of X-ray diffraction data collected in oscillation mode. Methods Enzymol. *276*, 307–326.

Pal, G.P., Elce, J.S., and Jia, Z. (2001). Dissociation and aggregation of calpain in the presence of calcium. J. Biol. Chem. *276*, 47233–47238.

Patrick, G.N., Zukerberg, L., Nikolic, M., de la Monte, S., Dikkes, P., and Tsai, L.H. (1999). Conversion of p35 to p25 deregulates Cdk5 activity and promotes neurodegeneration. Nature *402*, 615–622.

Richard, I., Broux, O., Allamand, V., Fougerousse, F., Chiannilkulchai, N., Bourg, N., Brenguier, L., Devaud, C., Pasturaud, P., Roudaut, C., et al. (1995). Mutations in the proteolytic enzyme calpain 3 cause limb-girdle muscular dystrophy type 2A. Cell *81*, 27–40.

Rizo, J., and Sudhof, T.C. (1998). C_2-domains, structure and function of a universal Ca^{2+}-binding domain. J. Biol. Chem. *273*, 15879–15882.

Santella, L., Kyozuka, K., De Riso, L., and Carafoli, E. (1998). Calcium, protease action, and the regulation of the cell cycle. Cell Calcium *23*, 123–130.

Sorimachi, H., and Suzuki, K. (2001). The structure of calpain. J. Biochem. *129*, 653–664.

Sorimachi, H., Ishiura, S., and Suzuki, K. (1997). Structure and physiological function of calpains. Biochem. J. *328*, 721–732.

Strobl, S., Fernandez-Catalan, C., Braun, M., Huber, R., Masumoto, H., Nakagawa, K., Irie, A., Sorimachi, H., Bourenkow, G., Bartunik, H., et al. (2000). The crystal structure of calcium-free human m calpain suggests an electrostatic switch mechanism for activation by calcium. Proc. Natl. Acad. Sci. USA *97*, 588–592.

Strynadka, N.C., Cherney, M., Sielecki, A.R., Li, M.X., Smillie, L.B., and James, M.N. (1997). Structural details of a calcium-induced molecular switch: X-ray crystallographic analysis of the calcium-saturated N-terminal domain of troponin C at 1.75 Å resolution. J. Mol. Biol. *273*, 238–255.

Thompson, J.D., Higgins, D.G., and Gibson, T.J. (1994). CLUSTAL W: improving the sensitivity of progressive multiple sequence alignment through sequence weighting, position-specific gap penalties and weight matrix choice. Nucleic Acids Res. *22*, 4673–4680.

Tompa, P., Baki, A., Schad, E., and Friedrich, P. (1996). The calpain cascade: μ-calpain activates m-calpain. J. Biol. Chem. *271*, 33161–33164.

Tompa, P., Emori, Y., Sorimachi, H., Suzuki, K., and Friedrich, P. (2001). Domain III of calpain is a Ca^{2+}-regulated phospholipid-binding domain. Biochem. Biophys. Res. Commun. *280*, 1333–1339.

Wang, K.K. (2000). Calpain and caspase: can you tell the difference? Trends Neurosci. *23*, 20–26.

Wang, K.K., and Yuen, P.W. (1994). Calpain inhibition: an overview of its therapeutic potential. Trends Pharmacol. Sci. *15*, 412–419.

Yoshizawa, T., Sorimachi, H., Tomioka, S., Ishiura, S., and Suzuki, K. (1995). Calpain dissociates into subunits in the presence of calcium ions. Biochem. Biophys. Res. Commun. *208*, 376–383.

Zimmerman, U.J., Boring, L., Pak, J.H., Mukerjee, N., and Wang, K.K. (2000). The calpain small subunit gene is essential: its inactivation results in embryonic lethality. IUBMB Life *50*, 63–68.

Accession Numbers

The structure coordinates can be accessed through the Protein Data Bank using the ID number 1KXR.